PCCP

Accepted Manuscript

This article can be cited before page numbers have been issued, to do this please use: S. Gallagher, A. Kavanagh, B. Ziolkowski, L. Florea, D. MacFarlane, K. Fraser and D. Diamond, *Phys. Chem. Chem. Phys.*, 2013, DOI: 10.1039/C3CP53397B.

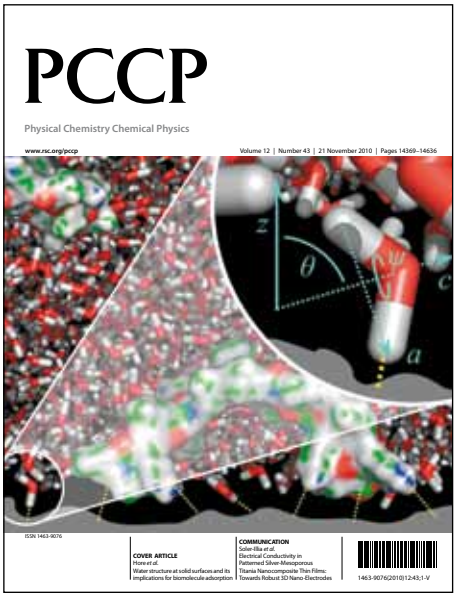

This is an *Accepted Manuscript*, which has been through the RSC Publishing peer review process and has been accepted for publication.

Accepted Manuscripts are published online shortly after acceptance, which is prior to technical editing, formatting and proof reading. This free service from RSC Publishing allows authors to make their results available to the community, in citable form, before publication of the edited article. This *Accepted Manuscript* will be replaced by the edited and formatted *Advance Article* as soon as this is available.

To cite this manuscript please use its permanent Digital Object Identifier (DOI®), which is identical for all formats of publication.

More information about *Accepted Manuscripts* can be found in the **Information for Authors**.

Please note that technical editing may introduce minor changes to the text and/or graphics contained in the manuscript submitted by the author(s) which may alter content, and that the standard **Terms & Conditions** and the **ethical guidelines** that apply to the journal are still applicable. In no event shall the RSC be held responsible for any errors or omissions in these *Accepted Manuscript* manuscripts or any consequences arising from the use of any information contained in them.

Dynamic Article Links ►
View Article Online
DOI: 10.1039/C3CP53397B

Cite this: DOI: 10.1039/c0xx00000x

www.rsc.org/pccp

PAPER

Ionic Liquid modulation of swelling and LCST behavior of *N*-isopropylacrylamide polymer gels.

Simon Gallagher[a], Andrew Kavanagh[a], Bartosz Zíołkowski[a], Larisa Florea[a], Douglas R. MacFarlane[b], Kevin Fraser[a] and Dermot Diamond[a]

Received (in XXX, XXX) Xth XXXXXXXXX 20XX, Accepted Xth XXXXXXXXX 20XX
DOI: 10.1039/b000000

Abstract

The physicochemical properties of free-standing cross-linked poly(*N*-isopropylacrylamide) (pNIPAAM) gels, generated in the presence of the Ionic Liquids (ILs), 1-ethyl-3-methylimidazolium $[C_2mIm]^+$ salts of ethylsulfate $[EtSO_4]^-$, dicyanamide $[DCA]^-$, *bis*(trifluoromethylsulfonyl)imide $[NTf_2]^-$, and Trihexyltetradecylphosphonium dycanamide ($[P_{6,6,6,14}][DCA]$) are described. The Lower Critical Solution Temperature (LCST) of the resulting ionogel was found to vary between 24 – 31 °C. The behaviour of swelling is found to be as high as 31.55% (± 0.47, n = 3) from the initial dehydrated state, while 28.04% (± 0.42, n = 3) shrinking from the hydrated swollen state is observed. For ionogels based on the $[DCA]^-$ anion an unexpected complete loss of the shrinking behaviour occurs, attributed to water interactions with the nitrile group of the $[DCA]^-$ anion. Scanning Electron Microscopy also reveals distinct morphological changes, for example $[C_2mim][EtSO_4]$ displays a highly porous, nodule type morphology, efficiently pre-disposed for water uptake.

Introduction

Hydrogels are porous, hydrophilic polymers capable of absorbing large amounts of water. The absorption process leads to bulk swelling, which is dependent on the polymeric chemical structure and the density of cross-linking agents [1]. Stimuli responsive hydrogels can actuate in the swollen state in response to external forces such as applied heat [2], a change in pH [3] or ionic strength [4], and incident electromagnetic fields [5].

One example of a well-studied thermally responsive hydrogel platform is poly(*N*-isopropylacrylamide) (pNIPAAM) [6]. In the presence of an aqueous solution, pNIPAAM displays inverse solubility properties upon heating above and below what is known as its Lower Critical Solution Temperature (LCST) [6, 7]. Experimentally, below the LCST, pNIPAAM is swelled with water through hydration of the polymerised aliphatic chain and hydrogen bonding interactions with its amide moiety, generating a gel network [8]. Above the LCST, the gel collapses along the polymer backbone before water molecules are expelled [9, 10]. This process is driven by a changeover from polymer-solvent interactions dominating at low temperatures to polymer-polymer and solvent-solvent interactions and structures dominating at the higher temperatures [6].

Ionic liquids (ILs) have received much attention over recent years, across diverse disciplines [11-13]. ILs commonly consist of a low symmetry organic cation and an inorganic / organic anion held together via weak electrostatic interactions, which reduce the lattice energy of the salt. This chemical environment (in most cases) contributes to factors such as negligible vapour pressures and generally high thermal stability [14, 15].

Three dimensional gel networks that are generated with the addition of ILs are known as ionogels. Ionogels are solid-state materials that retain unique IL properties, by allowing the IL to act as the liquid component of the gel. Recent reviews on the area [16-18], applications such as solid-state electrolytes [19, 20] and optical displays [21], are now available. Popular research avenues to date involving pNIPAAM are to improve the viscoelastic properties of the gels in its various states (initial, swollen and contracted) [22], modification of the LCST threshold to suit a given application [23] and liquid phase replacement which leads to mechanical issues, when volatile solvents are used [16]. LCST modifications have, however, been found to weaken and even eliminate the thermal sensitivity of the pNIPAAM-based hydrogels due to the introducing of the non-thermosensitive moiety [24].

The addition of ILs to the pNIPAAM network provides an opportunity to avoid these limitations, leading to stable responsive materials that have improved viscoelastic properties with modified LCST [9]. Compared to a traditional hydrogel, an ionogel was found to have greater thermal actuation, increased viscoelasticity, and induce a downshift in LCST to a more ambient 26 °C [25]. It is clear therefore, that the addition of the IL to the pNIPAAM network provides several advantageous routes toward the development of materials that improve some of the limitations of the traditional hydrogel model.

In this paper, we further investigate this triumvirate of interactions, namely, between the polymer network, and both independent liquid phases within the network (ILs and the absorbed water). This is achieved through variation of the IL phase within the material, ranging from water miscible to strongly alkylated materials. As ILs exhibit negligible vapour

View Article Online
DOI: 10.1039/C3CP53397B

pressure, these materials have the potential to be employed under open atmospheres with variable LCST. The mechanical and actuation properties of these thermally responsive ionogel materials are investigated, allowing for their continued functional use in important applications such as drug delivery [26], polyelectrolytes [27] and actuators [28].

Experimental

Chemical and Materials

N-isopropylacrylamide 98% (NIPAAM), *N,N'*-methylenebisacrylamide 99% (MBIS), Aluminum Oxide (activated, basic, Brockmann I), Potassium Bromide and 2,2-Dimethoxy-2-phenylacetophenone 98% (DMPA) were purchased from Sigma Aldrich® , Ireland and used as received. Trihexyltetradecylphosphonium dicyanamide $[P_{6,6,6,14}][DCA]$ (CYPHOS IL 105), was kindly donated by Cytec® Industries, Ontario, Canada. 1-ethyl-3-methylimidazolium ethyl sulphate $[C_2mim][EtSO_4]$ and 1-ethyl-3-methylimidazolium dicyanamide $[C_2mim][DCA]$ were supplied by Merck® industries. 1-ethyl-3-methylimidazolium *bis*(trifluoromethanesulfonyl)imide $[C_2mim][NTf_2]$ was synthesized via an ion-exchange methathesis reaction as previously described [29]. Materials used in this study are shown in Figure 1.

All ILs were column cleansed using aluminium (activated, basic, Brockmann I) with dichloromethane used as the mobile phase. This was then removed under vacuum at 40°C for 48 hrs at 0.1 Torr [30].

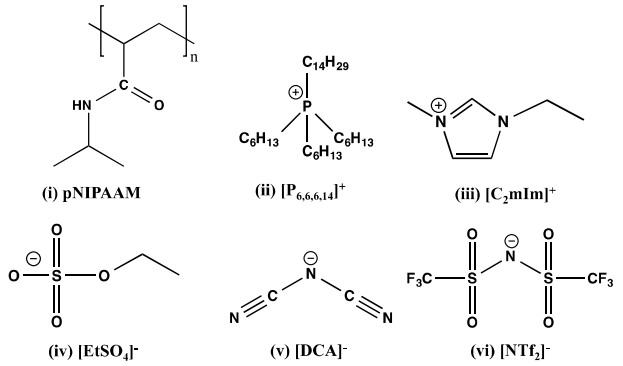

Figure 1. Molecular structures of the components used for the fabrication of an ionogel; (i) Poly(N-isopropylacrylamide), (ii) Trihexyl-tetradecylphosphonium $[P_{6,6,6,14}]^+$, (iii) 1-ethyl-3-methylimidazolium $[C_2mim]^+$, (iv) ethyl-sulfate $[EtSO_4]^-$, (v) dicyanamide $[DCA]^-$ and (vi) *bis*(trifluoromethanesulfonyl)imide $[NTf_2]^-$.

Preparation of Crosslinked Ionogels

pNIPAAM ionogels were prepared by mixing 400 mg of NIPAAM monomer (3.53 mmol), 27 mg of MBIS crosslinker (0.18 mmol), 18 mg photoinitiator (DMPA (0.07 mmol) (Final molar ratio 100:5:2), with 1.2 ml of the relevant IL. The mixture was heated to 50 °C and sonicated for 5 min. until a transparent solution was observed. Table 1 shows details of the compositions of mixtures studied and their abbreviations. 200 µL of the monomeric solution were then dispensed into a Teflon mould, 12 mm in radius, and photo-polymerized using a Connecticut 20 W UV Bond Wand set at 365 nm for 10 min [25]. The synthesized gels were immersed in distilled water for at room temperature for 48 hrs and the water was refreshed several times in order to allow the unreacted chemicals to leach out.

Preparation of Linear Homopolymers

Preparation of linear pNIPAAM homopolymers were synthesized in the absence of crosslinker MBIS, keeping all other experimental conditions the same as mentioned in the synthesis of crosslinked ionogels (Table 1). All resulting polymerized mixtures were dissolved in acetone. Then C-$EtSO_4$, C-DCA and the standard hydrogel were precipitated from water at 50 °C, while C-DCA and P-DCA were precipitated from diethyl ether. This process was repeated twice and the purified polymer was then dried in a vacuum oven at 50 °C, for 24 hours.

Sample Abbreviation	IL (1.2ml)	NIPAAM (mmol)	MBIS (mmol)	DMPA (mmol)
xC-$EtSO_4$	$[C_2mim][EtSO_4]$	3.53	0.18	0.07
C-$EtSO_4$	$[C_2mim][EtSO_4]$	3.53	-	0.07
xC-NTf_2	$[C_2mim][NTf_2]$	3.53	0.18	0.07
C-NTf_2	$[C_2mim][NTf_2]$	3.53	-	0.07
xC-DCA	$[C_2mim][DCA]$	3.53	0.18	0.07
C-DCA	$[C_2mim][DCA]$	3.53	-	0.07
xP-DCA	$[P_{6,6,6,14}][DCA]$	3.53	0.18	0.07
P-DCA	$[P_{6,6,6,14}][DCA]$	3.53	-	0.07

Table 1. Abbreviations and compositions of samples used in this study.

Details of the characterisation techniques used throughout this work can be found in the accompanying supplementary information.

Results and Discussion

Swelling and Shrinking Properties

Table 2 is a summary of the individual LCST thresholds, % swelling increase from the dehydrated state and % contractions from the fully hydrated state recorded for all ionogels. As a control experiment, the same parameters for a conventional hydrogel were also recorded.

View Article Online
DOI: 10.1039/C3CP53397B

Table 2. 1: Increase in disc diameter (a) from dehydrated state to fully hydrated state at T = 20 °C (n = 3). 2: Decrease in disc diameter (b) from fully hydrated state (a) when T = 40 °C (n = 3). Initial diameter in the dehydrated state is 12 mm for all gels. Tacticity determined by ^{1}H NMR at 120 °C (meso (m) and racemo (r) dyads).

Ionogel	LCST (°C)	Tacticity (m/r)	Swollen Diameter/mm (n=3)	% Swelling Increase (a)	Contracted Diameter/mm (n=3)	% Contraction Decrease (b)
xC-$EtSO_4$	26	52/48	15.71 (± 0.18)	30.9 (± 0.69)	11.3 (± 0.26)	28.04 (± 0.42)
xC-NTf_2	24	50/50	13.9 (± 0.17)	15.83 (± 0.85)	12.02 (± 0.06)	13.51 (± 0.63)
xC-DCA	-	47/53	15.78 (± 0.24)	31.55 (± 0.47)	-	-
xP-DCA	31	45/55	15.3 (± 0.11)	27.5 (± 0.66)	-	-
Hydrogel	32	47/53	14.23 (± 0.21)	18.6 (± 0.92)	11.47 (± 0.2)	19.38 (± 0.72)

All samples were prepared using the same monomer, cross-linker and photoinitiator ratios (100:5:2). As with previous studies, the liquid phase is the only experimental variant in all cases [25, 31] thus all physical parameters recorded are a function of the unique chemical environment of the solvent employed. It was noted that the extent of swelling for most ionogels was greater than the hydrogel control, with xC-NTf_2 being the notable exception. The degree of shrinking was less in all cases however, with xC-$EtSO_4$ being the exception, and interestingly, no LCST behaviour for ionogels based on the $[DCA]^-$ anion was apparent.

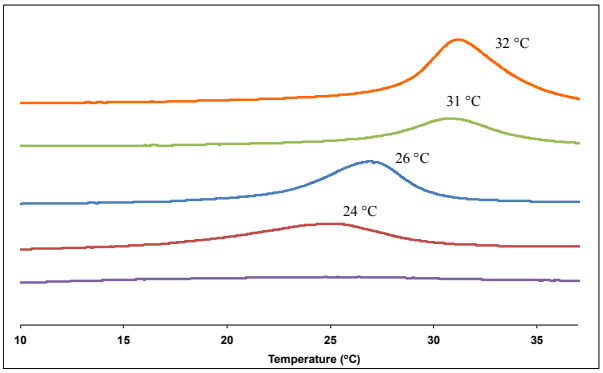

Figure 2. Thermal scans showing endothermic LCST transitions of hydrated pNIPAAM-gels, (orange) hydrogel, (green) xP-DCA, (blue) xC-$EtSO_4$, (red) xC-NTf_2, (purple) xC-DCA.

Figure 2 is an overlay of the thermal LCST behaviour for all ionogels and the hydrogel sample, as measured using differential scanning calorimetry. In Figure 2, all ionogel LCST parameters obtained, apart from xP-DCA, were found to deviate from the pNIPAAM literature value (31 °C) [6], with a range from 24 to 31 °C observed.

It has been reported that phase transition temperatures, swelling and shrinking properties of the crosslinked pNIPAAM gels have varied as a function of the isotacticity of their corresponding pNIPAAM homopolymers [32, 33]. The degree of isotacticity of the polymer chain segment is estimated by calculating the proportion of meso (m) and racemo (r) dyads from the region of the backbone methylene protons at ~1.2 – 1.8 ppm. With an increase in isotacticity, interactions among side-chain functional groups of the polymer become stronger, leading to less interaction with water and a decrease in the hydrophilicity of the polymer. This decrease of interactions between the side groups and water has been found to increase swelling, decrease shrinking and lower the pNIPAAM phase transition temperature [32, 33].

To investigate the effect of the IL on the tacticity of the pNIPAAM chain segment, ^{1}H NMR spectroscopy was carried out on the corresponding linear homopolymers. Isotacticity values were determined from Figure S1. The isotacticity (m) is calculated by the fraction of the meso dyads equal to the twice of its peak area divided by the peak areas of all three methylene peaks in the region (Table 2). In the absence of an IL, the conventional hydrogel with an isotacticity m = 47 %, is formed in ethanol:water (1:1, v/v). C-$EtSO_4$ and C-NTf_2 are found to have a higher isotacticity m = 52 and 50 %, respectively. These isotacticity values are found to correlate with the hydrogel phase transition temperature at 32 °C. This is consistent with previous reports, which have also found higher isotacticity to associated with lower pNIPAAM LCST [33]. Both ionogels studied have a lower LCST than the standard hydrogel, with xC-$EtSO_4$ and xC-NTf_2 occurring at 26 °C and 24 °C, respectively. However, a clear trend in the swelling and shrinking properties of the ionogels cannot be directly correlated with the isotacticity values obtained for the linear polymers. This is due the effect of the hydrophilic character of the IL itself which clearly can exert a substantial influence on the swelling and shrinking properties of the resulting pNIPAAM ionogels; i.e. water uptake and release behaviour is dominated by the hydrophilicity of the polymerization medium rather than the tacticity of the polymer chain segment formed.

Infrared Spectroscopy has been used successfully to determine the correlation between the LCST behaviour and amide interactions via the intramolecular hydrogen bonded N-H band (1551 cm^{-1}) [34, 35]. These interactions were studied on the ionogels when hydrated, with respect to the standard hydrogel (initial and hydrated states). Table 3 provides a summary of the IR analysis of all hydrated ionogels and the spectra can be found in Figure S2.

The amide II band representing the N-H group of the standard hydrogel is located at 1550 cm^{-1} (Figure S2), while the hydrated hydrogel shows a shift of 5 cm^{-1} to 1555 cm^{-1} with respect to the dry hydrogel. However, in contrast, the ionogels show a much larger shift when hydrated, with xC-$EtSO_4$ and xC-NTf_2 undergoing a shift of 10 and 12 cm^{-1}, respectively. With a LCST of 24 °C, xC-NTf_2, shows a greater shift than xC-$EtSO_4$, which has a LCST of 26 °C. It has been found that addition of the IL leads to weakening of hydrogen bonding between polymer and water molecules [9]. The results in Figure S2, suggest that, when hydrated, the IL's increased interaction with the amide group of the polymer results in a decrease in polymer/ water interactions leading to less energy input needed to allow a hydrophobic collapse, and therefore a lower

View Article Online
DOI: 10.1039/C3CP53397B

temperature to reach the phase transition.

Sample	ν (cm^{-1})	Δ ν (cm^{-1})	LCST (°C)
Hydrogel	1550	-	-
Hydrated Hydrogel	1555	**5**	**32**
Hydrated xC-$EtSO_4$	1560	**10**	**26**
Hydrated xC-NTf_2	1562	**12**	**24**
Hydrated xC-DCA	1560	**10**	**-**
Hydrated xP-DCA	1550	**-**	**31**

Table 3. Summary of the wavenumber positioning from infrared spectroscopy for the amide II band of various hydrated gels.

It is notable that there is a shift in the amide II band for xC-DCA, however, it does not show an LCST transition, nor any shrinking behaviour. While xP-DCA does not display any shift in the amide II band, but yet also exhibits no shrinking behaviour. This implies that there is more to the LCST than the amide interactions suggest. To investigate this and the high variation in swelling and shrinking behaviour further, a deeper understanding of the thermally dependent physicochemical processes is required, beginning with ionogels of the $[DCA]^-$ anion.

Ionogels based on the $[DCA]^-$ anion

In order to gain an insight into the liquid phase activity of the ionogel, we performed an independent physicochemical study centred on IL/H_2O interactions over the temperature range corresponding to the LCST behaviour. Karl-Fischer, temperature dependence of viscosity and density showed [C2mIm][DCA] exhibited high water miscibility, manifesting in a high viscosity change (93.43%, Figure 3) but little deviation in density at 20 °C (Tables S1, S2).

As the ionogel is essentially anhydrous at the onset, there is large chemical potential for swelling in the presence of water, with the gel swelling by 31.55 % from the initial dehydrated state (See Table 2). The ionogel exhibited no LCST transition and did not contract as the temperature was raised which is in accordance with the DSC data that shows that no transition over the temperature range 10 - 50 °C.

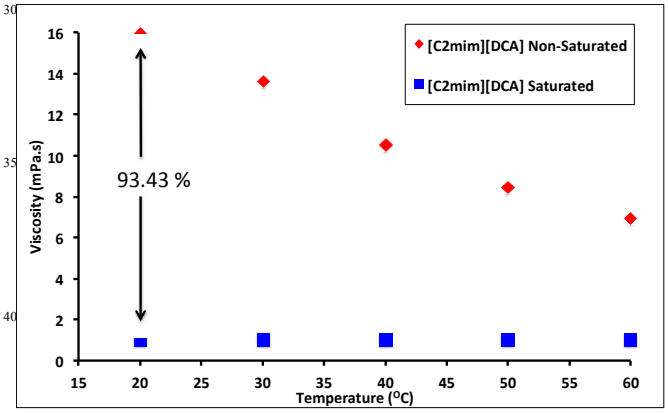

Figure 3. Viscosity values obtained for [C_2mim][DCA], dry **(red)** and water saturated **(blue)** as a function of temperature.

To investigate this phenomenon further, a more hydrophobic ionogel based on $[DCA]^-$ was prepared. In the $[P_{6,6,6,14}]^+$ cation the phosphonium charge centre is well shielded by long-chain alkyl groups, which leads to less interaction with water molecules [36]. Not surprisingly therefore, [$P_{6,6,6,14}$][DCA] is less miscible with water (mole fraction 0.43 x_w, Table S1), leading to little change in viscosity and density at 20 °C (Table S2). The xP-DCA ionogel was found to swell by 27.5 % from the initial dehydrated state, but like xC-DCA, no contraction occurred above the LCST (31 °C) (Table 2).

It appears that this unusual behaviour is an anionic effect, and given the nature of the materials under question, vibrational spectroscopy was again used to examine interactions at the molecular level. The nitrile stretch of the $[DCA]^-$ anion is well known to absorb in the infrared region, with the absorbance wavelength sensitive to strong molecular interactions, such as metal ion co-ordination [37]. Figures 4 and 5 provide a summary of the individual IR spectra for both $[DCA]^-$ based ionogels in the nitrile region.

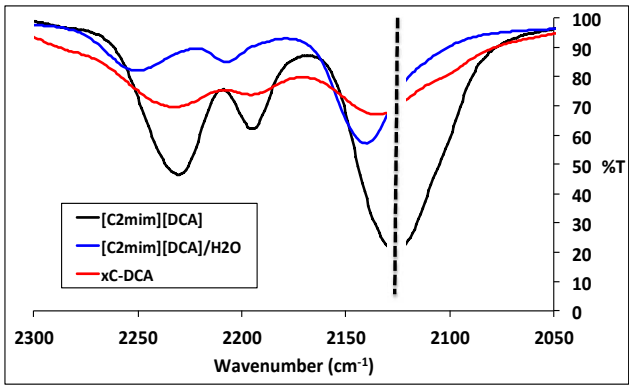

Figure 4. Infra-red spectroscopy recorded between 2050-2300 cm^{-1} of [C_2mim][DCA] (black), [C_2mim][DCA]: H_2O, 1:1 (v/v) (blue), and xC-DCA (red).

Analysis of the IL, the IL/water mixture and the ionogel (IL/polymer) was performed in each case, to investigate the IL/anion interactions with both water and the polymer. In Figure 4, the asymmetric nitrile stretch for [C_2mim][DCA] is located at 2127cm^{-1}, whilst with the non-hydrated ionogel (IL/polymer) and IL/H_2O (1:1 v/v) stretches are shifted significantly by 10 and 18 cm^{-1}, respectively.

The nitrile stretch of [$P_{6,6,6,14}$][DCA] is shown at 2128 cm^{-1}, with the respective IL/polymer and IL/H_2O interactions inducing spectral shifts to a lesser degree (most likely due to the increased IL hydrophobicity in this case).

From these findings, it can be postulated that dominating molecular interactions between the $[DCA]^-$ anion and its co-constituents, mainly water, serve to act as a competing stabilising influence, thereby inhibiting the LCST contraction mechanism. Consequently, no shrinking of the ionogel is observed, as the absorbed water is retained and the swollen state maintained at elevated temperatures (up to 45 °C). A summary of the wavenumber positioning of the asymmetric nitrile stretch of various $[DCA]^-$ IR spectral shifts are presented in Table 4.

View Article Online
DOI: 10.1039/C3CP53397B

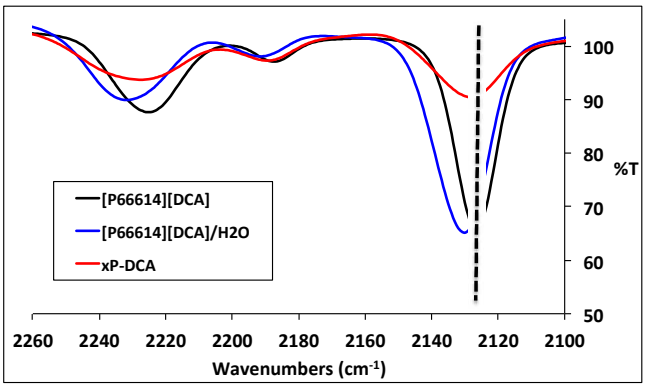

Figure 5. Infra-red spectroscopy recorded between 2100 and 2260 cm^{-1} for $[P_{6,6,6,14}][DCA]$ (black), $[P_{6,6,6,14}][DCA]$: H_2O mixture (blue). xP-DCA (red).

An interesting aspect of pNIPAAM is its contrasting surface topographies as the preparation solvent is varied [38]. Distinct features on the micron scale have been reported with respect to the formulation solvent used [39], and with the use of pore-forming agents, such as poly(ethyleneglycol) [40]. Figure S3 illustrates the changes in surface morphology associated with water uptake and swelling in a standard hydrogel [25].

Sample	ν (cm^{-1})	Δ ν (cm^{-1})
$[C_2mim][DCA]$	2127	-
$[C_2mim][DCA]$: H_2O (1:1, (v/v))	2145	**18**
xC-DCA	2137	**10**
$[P_{6,6,6,14}][DCA]$	2128	-
$[P_{6,6,6,14}][DCA]$: H_2O mixture	2131	**3**
xP-DCA	2130	**2**

Table 4. Summary of the wavenumber positioning from infrared spectroscopy for the asymmetric nitrile stretch of various $[DCA]^-$ IL samples.

Figure 6 demonstrates similar solvent dependent behaviour for the $[DCA]^-$ ionogels studied, in their swollen states. The effect of the IL is clear as the xC-DCA sample (water miscible, 31.55% swelling) exhibits a saturated pore free exterior, in contrast to the xP-DCA sample (0.428 x_w, 27.5% swelling), which appears less stressed, more fibrous, with visible signs of pores even after hydration.

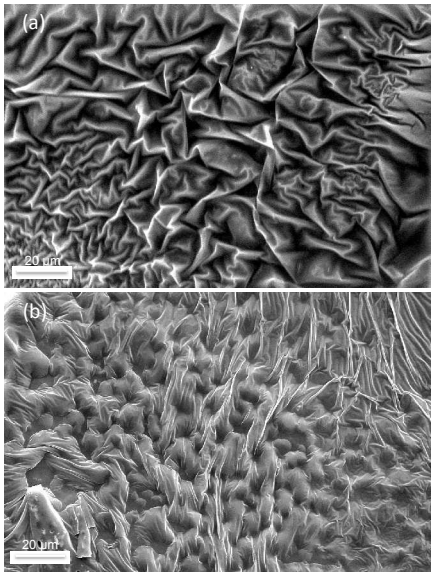

Figure 6. SEM images of swollen ionogels based on $[DCA]^-$. (a) xC-DCA and (b) xP-DCA

Enhanced Viscoelastic Ionogels

As previously described, a primary research avenue of pNIPAAM explored thus far is the improvement of the bulk viscoelastic properties, which have been shown to be unfavourable in some circumstances, due to the volatility of the gelated liquid phase [41]. Co-polymerised ionic surfactants have been shown to stabilise the viscoelasticity of pNIPAAM at a fixed cross-linking density through micellular aggregation, [4, 42]. For viscoelastic materials, the general mechanical properties are often characterised via the storage and loss moduli [31]. The storage modulus is related to the elastic energy of the hydrated gel as it contracts, whilst the loss modulus is the energy dissipated as heat flow from the gel [43]. The viscoelastic properties of xC-$EtSO_4$, xC-NTf_2, and a hydrogel equivalent are presented as a function of time and temperature in Figures 7 and S4.

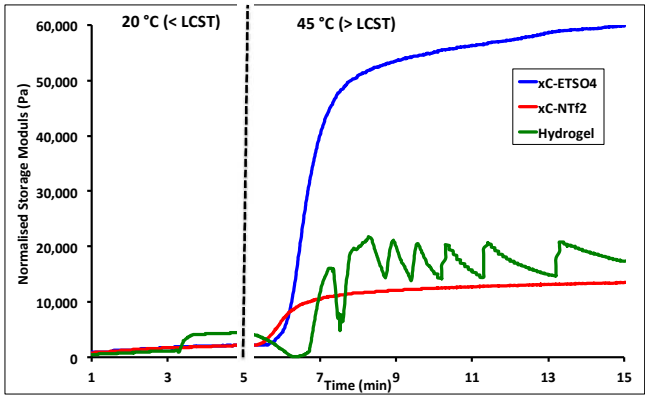

Figure 7. Storage modulus of (**blue**) xC-$EtSO_4$, **(red)** xC-NTf_2, and hydrogel **(green)**, plotted against time during a temperature ramp from 20 ºC to 45 ºC at 20 ºC / min.

View Article Online
DOI: 10.1039/C3CP53397B

Initially (0 to 5 min), all samples are in their hydrated states below the LCST (20 °C), and the shear frequency is kept constant. It can be seen from Figure 7 that both ionogels exhibit a stable mechanical response over this time period. Under the same experimental conditions the brittle hydrogel's mechanical stability is sporadic and fluctuates across a ~3,000 Pa range. At *t = 5 min*, the sample plate is heated from 20 to 45 °C, ensuring that any thermally sensitive processes related to the LCST are completed. As the temperature is increased, the storage modulus increases as the polymer contracts and its mechanical energy is stored internally in response to the applied stress. The sharp peaks produced by the hydrogel are due to the instrument readjusting the normal force on the sample. As the sample shrinks and changes modulus the reaction force of the sample drops and the instrument corrects for this (as described in the experimental section – see ESI) [40, 44]. The increase in the storage modulus of the hydrogel is erratic at higher temperatures, which reflects the material's inability to maintain the stored energy as it contracts, indicative of a material with fragile mechanical stability [43]. In contrast, the ionogel responses for the same experimental parameters plateau smoothly. Thus the ionogel template yields a more energetically stable contracted gel compared to the hydrogel under these conditions. The corresponding loss moduli of both gel platforms were found to correlate with the temperature dependent storage moduli features (Figure S4). Thus, from the rheological effects described, both ionogels xC-$EtSO_4$ and xC-NTf_2 display improved viscoelastic properties compared to the hydrogel. Significantly, this means that a relatively high density of cross-linking sites can exist within a yet flexible ionogel material. For the experiment depicted in Figure 7, the rheological features are consistently higher for xC-$EtSO_4$ over xC-NTf_2, indicating superior viscoelastic traits, which correlates well with the observed swelling and contracting behaviour (Table S2).

To differentiate the deviation in ionogel behaviour further, Raman spectroscopy was used to investigate the symmetrical – SO_3^- stretch commonly found in [C_2mim][$EtSO_4$] (Figure S5). The sulfoxide stretch of the IL is located at 1022 cm^{-1} [45]. The Raman spectrum of an aqueous phase aliquot released via LCST actuation contains the same sulfoxide stretch, although it is slightly shifted to 1025 cm^{-1} (Figure S5). Also, in 1:1 (v/v) mixtures of H_2O and IL, Karl-Fischer analysis shows [C_2mim][$EtSO_4$] to be miscible with water, while [C_2mim][NTf_2] is found to contain a mole fraction of 0.22 x_w of water (Table S1). This provides evidence that [C_2mim][$EtSO_4$], is expelled with the liquid phase through hydrogen bonding as the xC-$EtSO_4$ undergoes LCST phase transition. The release of IL, as well as absorbed water, causes a further decrease in polymer-solvent interactions, and an increase in polymer-polymer interactions, leading to a more compact format of the gel. In contrast, no evidence of [C_2mim][NTf_2] was found in the released aqueous phase from the xC-NTf_2 ionogel (Figure S6).

Figure 8 shows the morphology of the ionogels xC-NTf_2 and xC-$EtSO_4$ in their initial dehydrated and swollen states. Similar to the results presented in Figure 6, the presence of different ILs in the polymer matrix appears to have a significant effect on the surface topography.

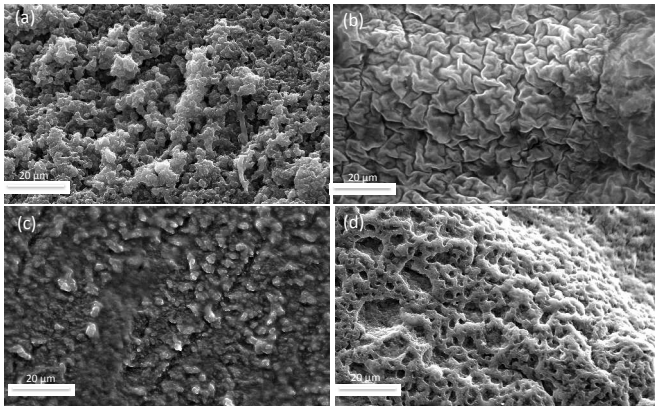

Figure 8. SEM images of xC-$EtSO_4$, after (a) polymerisation and (b) after swelling, and xC-NTf_2, after (c) polymerisation and (d) after swelling. Both ionogels were swelled in deionised water.

Figure 8 (a) and (c) show clear changes in the non-hydrated ionogel surface as the solvent used to prepare the ionogel is varied. The ionogel based on [C_2mim][$EtSO_4$] displays a highly porous, nodule type morphology, efficiently pre-disposed for water uptake, which changes further as it swells (Figure 8, (b)). The ionogel based on [C_2mim][NTf_2] exhibits hydration dependent surface features (Figure 8, (d), although the topography is less nodular when non-hydrated and is less compact in the swollen state.

The morphology in the dehydrated state of both ionogels indicates that the polymer is obtained in its more collapsed state (globular structure) rather than its common expanded coil. This is found to favour shrinking behaviour, which is supported by results found in Table 2 (% contraction).

Conclusions

Compared to a traditional freestanding pNIPAAM hydrogel the LCST of a range of imidazolium and phosphonium based ionogels varied between 24 – 31 °C. Each IL dictates a unique LCST value, xP-DCA being the highest (31 °C) and xC-NTf_2 being the lowest (24 °C). Actuation behaviour of the ionogel based on [C_2mim][$EtSO_4$] was found to be as large as 30.09% (± 0.69, n = 3) from the hydrated swollen state, while contraction from the swollen hydrated state was found to be 28.04% (± 0.42, n = 3).

For ionogels based on the $[DCA]^-$ anion an unexpected loss of the contraction behaviour occurs. Competing interactions involving the $[DCA]^-$ anion with water (specifically the nitrile stretch) were found to prevent a LCST triggered contraction, despite the initial high levels of swelling ([C_2mIm][DCA]: 31.55 % ± 0.47, n = 3).

Polymer rheology confirmed that whilst the actuation behaviour varies, the viscoelasticity of these ionogels is far greater and more stable than the hydrogel equivalent at the same cross-linker density. At this concentration of crosslinking (5 mol%), a flexible material is still obtained providing a suitable environment for combining high mechanical stability and actuation.

Scanning Electron Microscopy also reveals distinct morphological changes between ionogels and a standard

View Article Online
DOI: 10.1039/C3CP53397B

hydrogel, for example [C_2mim][$EtSO_4$] displays a highly porous, nodule type morphology, efficiently pre-disposed for water uptake. As a result of this study it is clear that there are well defined interactions between the polymer network, ILs and water that determine the "tailorability" of the ionogels such as the LCST and actuation behaviour.

Notes and references

We acknowledge support under the Marie Curie IRSES-MASK project (PIRSES-GA-2010-269302), Science Foundation Ireland grant (07/CE/I1147), Marie Curie Actions re-integration grant PIRG07-GA-2010-268365 (for K.J.F) and the Irish Research Council. D.R.M. is grateful to the Australian Research Council for his Federation and Australian Laureate Fellowships. We also acknowledge the contribution of Dr. Gary Annat for performing viscosity measurements.

[a] *CLARITY, The Centre for Sensor Web Technologies, National Centre for Sensor Research, School of Chemical Sciences, Dublin City University, Dublin, Ireland. Tel: +353 1 700 5404; E-mail: Dermot.diamond@dcu.ie*
[b] *School of Chemistry, Monash University, Wellington Road, Clayton, 3800, Vic, Australia.*

† Electronic Supplementary Information (ESI) available: Analytical techniques, NMR purification data, density, viscosity, DSC data, SEM imaging, Ionogel rheometry and Vibrational spectroscopy results. See DOI: 10.1039/b000000x/

1. G. Gulten and G. Aysegul, *Industrial & Engineering Chemistry Research*, 2011, **50**.
2. M. R. Guilherme, R. d. Silva, A. F. Rubira, G. Geuskens and E. C. Muniz, *Reactive and Functional Polymers*, 2004, **61**.
3. J. Hee Kyung, K. So Yeon and L. Young Moo, *Polymer*, 2001, **42**.
4. T. Friedrich, B. Tieke, F. J. Stadler and C. Bailly, *Soft Matter*, 2011, **7**, 6590-6597.
5. M. Molina, C. Rivarola, M. Miras, D. Lescano and C. Barbero, *Nanotechnology*, 2011, **22**, 245504.
6. H. G. Schild, *Progressive Polymer Science*, 1992, **17**, 163-249.
7. T. Ueki and M. Watanabe, *Chemistry Letters*, 2006, **35**.
8. T. Ueki, A. Yamaguchi, N. Ito, K. Kodama, J. Sakamoto, K. Ueno, H. Kokubo and M. Watanabe, *Langmuir : the ACS journal of surfaces and colloids*, 2009, **25**, 8845-8853.
9. P. Reddy and P. Venkatesu, *The Journal of Physical Chemistry*, 2011, **115**, 4752-4759.
10. Z. Ahmed, E. Gooding, K. Pimenov, L. Wang and S. Asher, *The journal of physical chemistry. B*, 2009, **113**, 4248-4304.
11. K. Fukumoto, M. Yoshizawa and H. Ohno, *Journal of the American Chemical Society*, 2005, **127**, 2398-2399.
12. K. R. Seddon, A. Stark and M.-J. Torres, *Pure Applied Chemistry*, 2000, **72**, 2275-2287.
13. M.-C. Tseng and Y.-H. Chu, *Chemical communications (Cambridge, England)*, 2010, **46**, 2983-2985.
14. L. Vidal, M.-L. Riekkola and A. Canals, *Analytica chimica acta*, 2012, **715**, 19-60.
15. P. Wasserscheid and T. Welton, *Wiley Online Library*, 2003, **1**.
16. T. Ueki and M. Watanabe, *Macromolecules*, 2008, **41**, 11.
17. A. Kavanagh, R. Byrne, D. Diamond and K. J. Fraser, *Membranes*, 2012, **2**, 16-55.
18. J. Le Bideau, L. Viau and A. Vioux, *Chemical Society reviews*, 2011, **40**, 907-932.
19. A. Kavanagh, R. Copperwhite, M. Oubaha, J. Owens, C. McDonagh, D. Diamond and R. Byrne, *Journal of Materials Chemistry*, 2011, **21**, 8687.
20. D. Khodagholya, V. F. Curto, K. J. Fraser, M. Gurfinkel, R. Byrne, D. Diamond, G. G. Malliaras, F. Benito-Lopez and R. M. Owens, *Journal of Materials Chemistry*, 2012, **22**, 4440-4443.
21. K. Lunstroot, K. Driesen, P. Nockemann, K. Van Hecke, L. Van Meervelt, C. Görller-Walrand, K. Binnemans, S. Bellayer, J. Le Bideau and A. Vioux, *Chemistry Materials*, 2006, **18**, 5711-5715.
22. K. Anseth, C. Bowman and L. Brannon-Peppas, *Biomaterials*, 1996, **17**, 1647-1704.
23. H.-N. Lee and T. Lodge, *The Journal of Physical Chemistry. B*, 2011, **115**, 1971-1977.
24. W. Xue and I. Hamley, *Polymer*, 2002, **43**.
25. S. Gallagher, A. Kavanagh, L. Florea, D. R. MacFarlane, K. Fraser, J. and D. Diamond, *Chemical Communications*, 2013, **49**, 4613-4615.
26. F. Yhaya, J. Lim, Y. Kim, M. Liang, A. M. Gregory and M. H. Stenzel, *Macromolecules*, 2011, **44**, 8433-8445.
27. S. Amajjahe, S. Choi, M. Munteanu and H. Ritter, *Angewandte Chemie (International ed. in English)*, 2008, **47**, 3435-3442.
28. H. Suzuki, *Journal of Intelligent Material Systems and Structures*, 2006, **17**.
29. L. Li, J. Wang, T. Wu and R. Wang, *Chemistry (Weinheim an der Bergstrasse, Germany)*, 2012.
30. M. Earle, J. Esperanca, M. Gilea, J. Lopes, L. Rebelo, J. Magee, K. Seddon and J. Widegren, *Nature*, 2006, **439**, 831-834.
31. B. Ziolkowski, Z. Ates, S. Gallagher, R. Byrne, A. Heise, K. Fraser, J. and D. Dermot, *Macromolecular Chemistry and Physics*, 2013.
32. C. Biswas, N. Vishwakarma, V. Patel, A. Mishra, S. Saha and B. Ray, *Langmuir : the ACS journal of surfaces and colloids*, 2012, **28**, 7014-7022.
33. C. Biswas, V. Patel, N. Vishwakarma, A. Mishra, S. Saha and B. Ray, *Langmuir : the ACS journal of surfaces and colloids*, 2010, **26**, 6775-6782.
34. Z. Xian-Zheng, Y. Yi-Yan, C. Tai-Shung and M. Kui-Xiang, *Langmuir*, 2001, **17**.
35. L. Shan-Yang, C. Ko-Shao and R. C. Liang, *Polymer*, 1998, **40**, 2619-2624.
36. M. S. S. N. Catarina, J. C. Pedro, G. F. Mara and A. P. C. Jo√£o, *The Journal of Chemical Thermodynamics*, 2011, **43**.
37. L. Ficke and J. Brennecke, *The journal of physical chemistry. B*, 2010, **114**, 10496-10501.
38. Z. Xian-Zheng, X. Xiao-Ding, C. Si-Xue and Z. Ren-Xi, *Soft Matter*, 2008, **4**.
39. A. Suk-kyun, M. K. Rajeswari, K. Seong-Cheol, S. Nitin and Z. Yuxiang, *Soft Matter*, 2008, **4**.
40. S. Hashmi, A. GhavamiNejad, F. O. Obiweluozor, M. Vatankhah-Varnoosfaderani and F. J. Stadler, *Macromolecules*, 2012, **45**, 9804-9815.
41. J. P. Gong, Y. Katsuyama, T. Kurokawa and Y. Osada, *Advanced Materials*, 2003, **15**.

View Article Online
DOI: 10.1039/C3CP53397B

42. T. Friedrich, B. Tieke, F. J. Stadler, C. Bailly, T. Eckert and W. Richtering, *Macromolecules*, 2010, **43**, 9964-9971.
43. P. C. Hiemenz and T. P. Lodge, *Polymer Chemistry, Second Edition*, CRC Press; 2 edition, Florida, 2007.
44. B. Ziółkowski, Z. Ates, S. Gallagher, R. Byrne, A. Heise, K. J Fraser and D. Diamond, *Macromolecular Chemistry and Physics (accepted)*, 2013, **214**, 787-796.
45. J. Kiefer, J. Fries and A. Leipertz, *Applied spectroscopy*, 2007, **61**, 1306-1311.

View Article Online
DOI: 10.1039/C3CP53397B

The lower critical solution temperature of cross-linked ionogels, containing the 1-ethyl-3-methylimidazolium ($[C_2mIm]^+$) and Trihexyltetradecylphosphonium($[P_{6,6,6,14}]^+$) cations are investigated. For ionogels based on the $[C_2mIm][DCA]$ IL, unexpected loss of the LCST occurs, attributed to water interactions with the nitrile stretch of the $[DCA]^-$ anion. Scanning Electron Microscopy also reveals distinct morphological changes before and after hydration between ionogels.